

RefDrone: A Challenging Benchmark for Referring Expression Comprehension in Drone Scenes

Zhichao Sun¹, Yepeng Liu¹, Huachao Zhu¹, Yuliang Gu¹, Yuda Zou¹, Zelong Liu¹
 Gui-Song Xia¹, Bo Du¹, Yongchao Xu^{1*}
¹School of Computer Science, Wuhan University

Abstract

Drones have become prevalent robotic platforms with diverse applications, showing significant potential in Embodied Artificial Intelligence (Embodied AI). Referring Expression Comprehension (REC) enables drones to locate objects based on natural language expressions, a crucial capability for Embodied AI. Despite advances in REC for ground-level scenes, aerial views introduce unique challenges including varying viewpoints, occlusions and scale variations. To address this gap, we introduce RefDrone, a REC benchmark for drone scenes. RefDrone reveals three key challenges in REC: 1) multi-scale and small-scale target detection; 2) multi-target and no-target samples; 3) complex environment with rich contextual expressions. To efficiently construct this dataset, we develop RDAgent (referring drone annotation framework with multi-agent system), a semi-automated annotation tool for REC tasks. RDAgent ensures high-quality contextual expressions and reduces annotation cost. Furthermore, we propose Number GroundingDINO (NGDINO), a novel method designed to handle multi-target and no-target cases. NGDINO explicitly learns and utilizes the number of objects referred to in the expression. Comprehensive experiments with state-of-the-art REC methods demonstrate that NGDINO achieves superior performance on both the proposed RefDrone and the existing gRefCOCO datasets. The dataset and code will be publicly at <https://github.com/sunzc-sunny/refdrone>.

1. Introduction

Drones/UAVs have become increasingly popular in our daily lives, serving both personal and professional purposes, such as entertainment, package delivery, traffic surveillance, and emergency rescue. Their ability to move freely and their broad observation capabilities make them important platforms for Embodied AI [6, 8, 17, 25, 27]. A crucial capability in Embodied AI is Referring Expression Com-

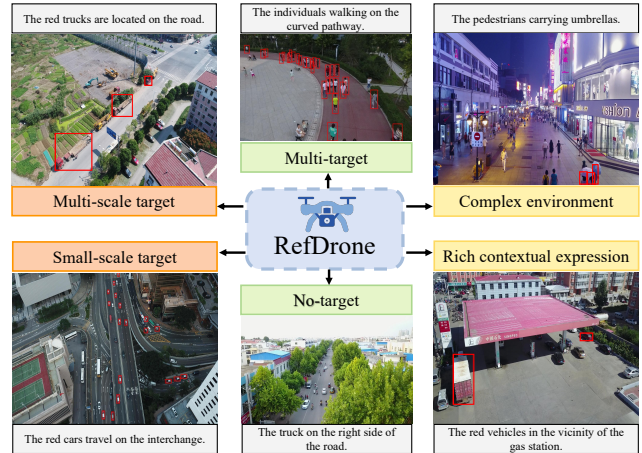


Figure 1. Examples of the various challenges in RefDrone dataset.

prehension (REC) [2, 35, 39, 40], which serves as a critical bridge between natural language understanding and visual perception. REC requires drones to localize specific objects in images based on natural language expressions. However, existing REC datasets primarily focus on ground-level perspectives, such as the RefCOCO [29, 45] dataset. The application of REC in drone-based scenarios presents unique challenges, including extreme viewpoint variations, occlusions, and scale variations across objects.

In this work, we introduce RefDrone, a challenging benchmark designed for REC in drone scenes. The RefDrone dataset contains 17,900 referring expressions across 8,536 images, comprising 63,679 object instances. As illustrated in Figure 1, RefDrone poses three key challenges that distinguish it from existing datasets: (1) multi-scale and small-scale target detection, with 31% small objects and 14% large objects; (2) multi-target and no-target samples, where expressions can refer to any number of objects from 0 to 242; and (3) complex environment with rich contextual expressions. The environmental complexity manifests in varied viewpoints, diverse lighting conditions, and complex backgrounds. The contextual richness is reflected in

*Corresponding author: yongchao.xu@whu.edu.cn

Table 1. Comparison of referring expression comprehension datasets: RefCOCO+/g [29, 45], gRefCOCO [22], D³ [42], RIS-CQ [13], RSVG [47], and RefDrone (ours). Avg. object: average number of objects per expression. Avg. length: words per expression. No target: expressions without referred objects. Expression type: expression generation method. Small target: small-scale target detection challenge.

	RefCOCO+/g [29, 45]	gRefCOCO [22]	D ³ [42]	RIS-CQ [13]	RSVG [47]	RefDrone
Image source	COCO [20]	COCO [20]	COCO [20]	VG [16]+COCO [20]	DIOR [18]	VisDrone [49]
Avg. object	1.0	1.4	1.3	3.6	2.2	3.8
Avg. length	3.6/3.5/8.4	4.9	6.3	13.2	7.5	9.0
No target	✗	✓	✓	✗	✗	✓
Expression type	Manual	Manual	Manual	LLM (GPT3.5-t)	Templated	LMM (GPT4-o)
Small target	✗	✗	✗	✗	✓	✓

expressions that describe spatial relations, attributes, and interactive relationships.

To efficiently construct this comprehensive dataset, we develop RDAgent (referring drone annotation framework with multi-agent system), a semi-automated annotation pipeline. RDAgent restructures traditional annotation workflows into an interactive system of multiple agents and human annotators. In this framework, agents with diverse roles collaborate through feedback loops to generate and verify annotations, while human involvement is minimized to quality control and minor adjustments. RDAgent significantly reduces annotation costs while maintaining high-quality standards for complex expressions, and it can be extended to generate annotations for other REC tasks.

Furthermore, we propose a novel method called Number GroundingDINO (NGDINO). Our key insight is that utilizing the number information of referred objects enhances the handling of multi-target and no-target samples. NGDINO comprises three key components: (1) a number prediction head that estimates target object quantities, (2) a set of learnable number-queries encoding numerical patterns across different quantity samples, and (3) a number cross-attention module that integrates number queries with detection queries. Extensive experiments on both our drone-specific RefDrone benchmark and the general-domain gRefCOCO [22] dataset reveal that leveraging the number information greatly improves performance on multi-target and no-target samples.

In summary, our contributions are listed as follows:

1. **RefDrone Benchmark:** The first comprehensive benchmark for referring expression comprehension in drone scenes. RefDrone poses three key challenges and provides comprehensive baseline evaluations across both specialized models and large multimodal models.
2. **RDAgent Annotation Framework:** A novel semi-automated annotation framework employs a multi-agent system. RDAgent reduces annotation costs while ensuring high-quality referring expressions.
3. **NGDINO Method:** A novel method specifically designed to handle multi-target and no-target samples through three components: a number prediction head,

learnable number-queries, and number cross-attention. NGDINO achieves superior performance on both RefDrone and gRefCOCO datasets.

2. Related works

2.1. Referring expression understanding datasets

Referring expression understanding identifies specific regions within images or videos using natural language expressions. Two primary subtasks are Referring Expression Comprehension (REC) and Referring Expression Segmentation (RES). REC outputs detection bounding boxes, while RES outputs segmentation masks. Early datasets such as ReferIt [15] and RefCOCO [45] are pioneering but are limited to single-target expressions and simple expressions. Subsequently, datasets [13, 22, 37, 42] introduce more challenges. gRefCOCO [22] supports multi-target expressions. OV-VG [37] enables an open-vocabulary setting. D³ [42] and RIS-CQ [13] introduce more complex expressions. Additionally, domain-specific datasets [30, 32, 47] emerge to address unique applications. RSVG [47] focuses on remote sensing, RAVAR [30] targets video action recognition, and RIO [32] addresses affordance detection. However, drone scenes remain unexplored in REC tasks, which motivates our introduction of the RefDrone benchmark.

Recent advances in dataset creation have been significantly influenced by large language models (LLMs). Notable works such as LLaVA [24] and Ferret [44] show the effectiveness of LLMs in generating instruction tuning data. Similarly, RIS-CQ [13] and RIO [32] employ LLMs to generate complex referring expressions. However, these approaches have two limitations. First, LLMs are used mainly as text generators, potentially producing expressions without proper grounding in visual context. Second, the lack of iterative feedback mechanisms in the annotation pipelines may degrade annotation quality.

2.2. Referring expression comprehension methods

Referring expression comprehension methods can be broadly categorized into specialist models and large multimodal models (LMMs). Specialist models include two-

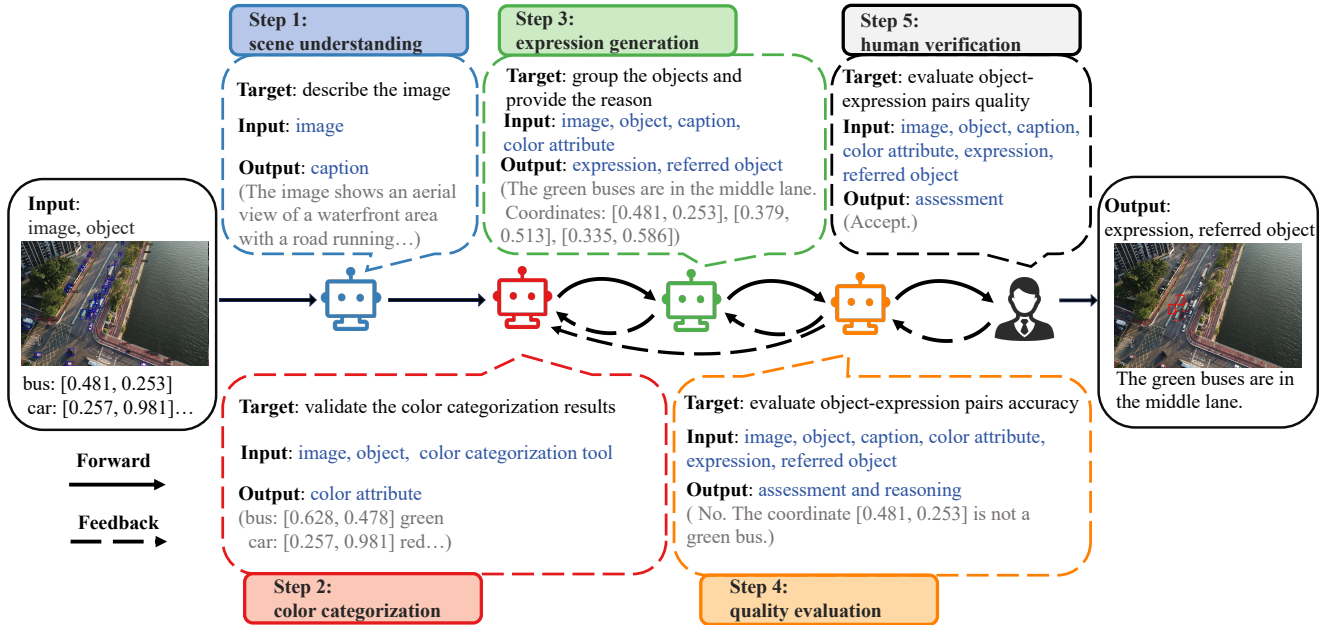


Figure 2. The overview of the RefDrone annotation process with RDAgent. Multiple specialized agents collaborate both with each other and human annotators through iterative feedback loops to generate high-quality annotations.

stage and one-stage methods. Two-stage methods [9, 10, 12, 23, 36] typically approach REC as a ranking task, first generating region proposals and then ranking them based on language input. However, they are often criticized for slow inference speeds. In contrast, one-stage methods [7, 14, 19, 26, 28, 43] directly predict target regions guided by language. These approaches leverage transformer architectures to enable cross-modal interactions between visual and textual features. Among these methods, GroundingDINO (GDINO) [28] has gained widespread attention for its impressive results in both open-set object detection and REC tasks. However, GDINO lacks explicit mechanisms to handle multi-target or no-target scenarios.

Recent studies have increasingly evaluated LMMs [1, 3, 5, 21, 24, 31, 38, 41, 44, 48] on REC tasks to assess their visual-language understanding capabilities. These models leverage large-scale referring instruction tuning data to achieve remarkable performance. Despite their broad capabilities, LMMs consistently struggle with small object detection, primarily due to their inherent input resolution constraints. This constraint forces image downsampling, resulting in the loss of fine-grained visual details.

3. RefDrone benchmark

3.1. Data source

The RefDrone dataset builds upon VisDrone2019-DET [49], a drone-captured dataset for object detection. The source images are collected across multiple scenarios,

illumination conditions, and flying altitudes. To ensure meaningful visual content, we implement two filtering criteria. At the image level, we exclude images containing less than 3 objects. At the object level, we exclude objects with bounding box areas below 64 pixels. The original VisDrone2019-DET annotations provide object categories and bounding box coordinates. We convert the bounding box to a normalized center point (range 0-1). This approach reduces the input context for LMMs while preserving spatial information.

3.2. RDAgent for semi-automated annotation

RDAgent (referring drone annotation framework with multi-agent system) is a semi-automated annotation framework that enhances traditional annotation pipelines by integrating LMMs with human annotators. Central to RDAgent are multiple LMM agents, specifically GPT-4o, each perform specialized tasks via distinct system prompts. As shown in Figure 2, RDAgent employs five structured steps.

Step 1: scene understanding. A GPT-4o-based captioning agent generates three diverse textual descriptions per image. These captions provide contextual perspectives (e.g., object relationships, spatial layouts) to anchor subsequent referring expression generation.

Step 2: color categorization. Color attributes serve as crucial discriminative features in referring expressions. Color attributes are extracted using a hybrid pipeline: (1) a WideResNet-101 [46] model trained on HSV color space-based labels, refined via manual validation, and (2) a ded-

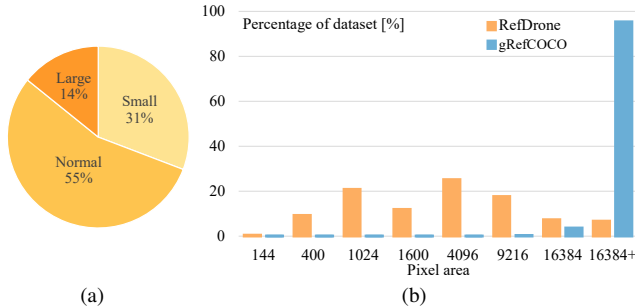


Figure 3. Object size distribution analysis. (a) Object size distribution in RefDrone dataset (small: $< 32^2 = 1024$ pixels, normal: 1024 to 9216 pixels, large: $> 96^2 = 9216$ pixels). (b) Object size histograms in RefDrone and gRefCOCO [22] datasets.

icated LMM agent that verifies predictions to mitigate illumination- or occlusion-induced errors.

Step 3: expression generation. To address the complexity in referring expression generation, we reformulate the referring expression generation task as an object grouping problem. The target of the agent is to group semantically related objects and to provide appropriate reasons for each group. The reasons serve as the referring expressions. Furthermore, a dynamic feedback loop triggers color categorization (Step 2) when novel colors are detected, ensuring color attribute consistency.

Step 4: quality evaluation. An evaluator agent assesses the annotation semantic accuracy and referential uniqueness of object-expression pairs, categorizing annotations as:

- “Yes.” The annotation is accurate and unique to the described objects.
- “No.” The annotation is inaccurate or non-unique, with a detailed explanation of the discrepancy.

Annotations marked “Yes” proceed to Step 5. Annotations marked “No” activate specific feedback: expressions with semantic issues are returned to Step 3 (expression generation), while color-related inaccuracies are sent to Step 2 (color categorization) for refinement.

Step 5: human verification. Human annotators review annotation outputs in three tiers:

- Direct acceptance. Annotations satisfying all quality criteria are approved for the final dataset.
- Refinement required. Annotations with minor errors are corrected through human editing.
- Significant issues. Annotations with major errors or unclear descriptions are marked for complete reworking.

Annotations with significant issues enter a feedback loop, returning to Step 4 (quality evaluation). If an annotation repeatedly fails to meet standards, it becomes a no-target sample. These feedback refinement loops ensure that all annotations meet our quality standards and that no-target expressions still relate to the image content.

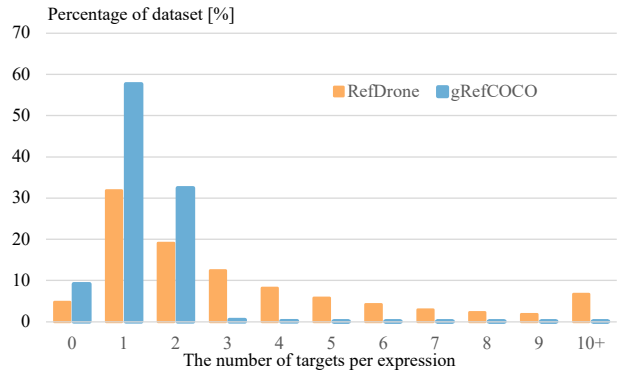


Figure 4. Object number distribution per expression in gRefCOCO [22] and RefDrone datasets.

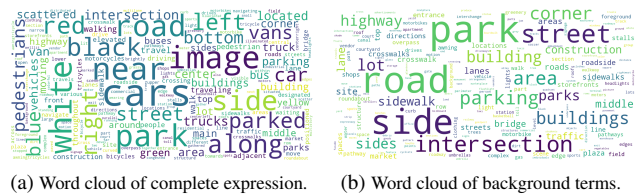


Figure 5. Word frequency visualization in RefDrone dataset.

Each step utilizes LMMs through in-context learning with manually designed prompts and examples (see Supplementary Material). RDAgent requires only \$0.0539 per expression in GPT4-o API cost and reduces human annotation effort by 88% compared to fully manual annotations. This cost-performance balance makes the framework scalable for large-scale datasets.

3.3. Dataset analysis

The RefDrone dataset contains 17,900 referring expressions across 8,536 images, comprising 63,679 object instances in 10 categories. We maintain the original train, validation, and test splits from VisDrone2019-DET [49]. The dataset features an average expression length of 9.0 words, with each expression referring to an average of 3.8 objects. Figure 1 gives several examples that relate to the three key features and challenges in RefDrone:

1) Multi-scale and small-scale target detection. Figure 3 presents an analysis of object scale distribution in RefDrone, with (a) showing the overall distribution and (b) offering a comparison with the gRefCOCO [22] dataset. In the RefDrone dataset, small-scale objects constitute 31% of all instances, while large-scale objects account for 14%. The detailed scale distribution in RefDrone demonstrates greater variance compared to gRefCOCO, highlighting the multi-scale challenges in RefDrone.

2) Multi-target and no-target samples. The RefDrone dataset includes 11,362 multi-target and 847 no-target ex-

pressions, with the number of referred targets ranging from 0 to 242. Figure 4 illustrates the target number distribution, revealing higher complexity in multi-target scenarios compared to gRefCOCO, where expressions typically refer to no more than two objects.

3) Complex environment with rich contextual expressions. The images present inherent complexity including diverse viewpoints, varying lighting conditions, and complex background environments. The referring expressions go beyond simple object attributes (*e.g.*, color, category) and spatial relationships (*e.g.*, ‘left’, ‘near’), incorporating rich object-object interactions (*e.g.*, ‘the white trucks carrying livestock’) and object-environment interactions (*e.g.*, ‘the white cars line up at the intersection’). Figure 5 presents word cloud visualizations of (a) complete expressions and (b) background terms, highlighting the diverse vocabulary used in descriptions.

3.4. Dataset comparison

Table 1 compares RefDrone with existing REC datasets. RefDrone stands out by its average number of referred objects and its use of LMM for expression generation. The expressions offer richer contextual details compared to template-based or human-annotated expressions. While RIS-CQ [13] employs LLM for expression generation, it lacks visual content during the generation process. This often results in expressions that, despite being linguistically complex, may be disconnected from visual content. Similarly, RSVG [47], although it focuses on small targets, falls short in terms of expression quality. In contrast, RefDrone comprehensively presents three challenges, establishing it as a challenging benchmark in REC tasks.

3.5. Evaluation metrics

We introduce instance-level metrics extending traditional REC metrics to address multi-target challenges. Previous benchmarks primarily focus on image-level metrics, which are sufficient for single-target or few-target samples. However, these metrics fail to handle expressions referring to multiple target objects—potentially scaling up to 100 instances per expression in our task. To address this limitation, we introduce instance-level metrics that provide a more granular evaluation of a model’s capability to identify individual target objects.

Instance-level metrics: $\text{Acc}_{inst.}$ and $\text{F1}_{inst.}$ measure the accuracy of individual bounding box predictions. We compute the intersection over union (IoU) between the true bounding boxes and the predicted bounding boxes. An $\text{IoU} \geq 0.5$ is considered a true positive (TP), otherwise it is a false positive (FP). Unmatched true bounding boxes are counted as false negatives (FN). For no-target samples, a prediction without any bounding box is a true negative (TN), otherwise it is a false positive (FP). We calculate:

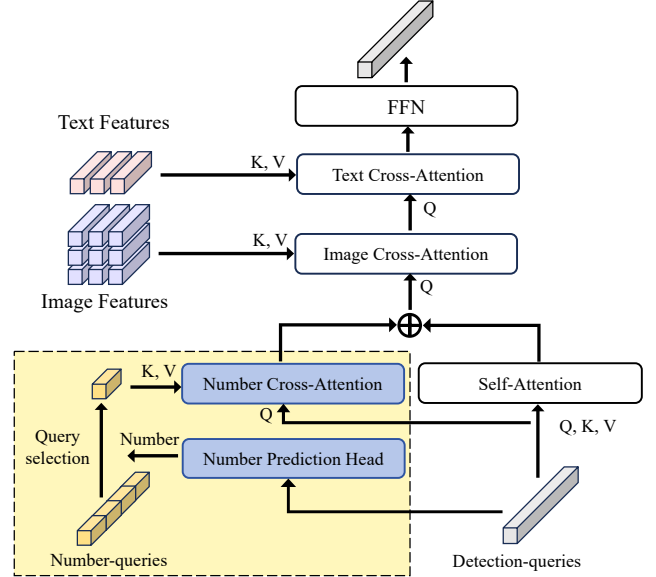


Figure 6. Architecture of a single decoder layer in Number GroundingDINO. Key modifications from GDINO [28] (highlighted in yellow box) include: (1) number prediction head (FFN) to predict target number, (2) number-queries selected through the predicted number, (3) number cross-attention between selected number-queries and detection-queries.

$$\text{Acc}_{inst.} = \frac{TP + TN}{TP + TN + FP + FN} \quad (1)$$

and

$$\text{F1}_{inst.} = \frac{2 \cdot TP}{2 \cdot TP + FP + FN} \quad (2)$$

Image-level metrics: $\text{Acc}_{img.}$ and $\text{F1}_{img.}$ evaluate the overall accuracy of predictions per image. An image is considered a true positive (TP) if all predictions match the true bounding boxes, otherwise it is a false positive (FP). For no-target samples, a prediction without any bounding box is a true negative (TN), otherwise it is a false positive (FP). We calculate $\text{Acc}_{img.}$ and $\text{F1}_{img.}$ using the same formulas as $\text{Acc}_{inst.}$ and $\text{F1}_{inst.}$, respectively.

4. Proposed method

We introduce Number GroundingDINO (NGDINO) to address multi-target and no-target challenges based on GDINO [28]. Our insight is that utilizing number information of referred objects enhances model performance on these challenges. As illustrated in Figure 6, we introduce three components: (1) a number prediction head, (2) number-queries, and (3) a number cross-attention module.

4.1. NGDINO

Following GDINO, our model employs a dual-encoder-single-decoder architecture. The framework consists of an

image backbone for visual feature extraction, a text backbone for text feature extraction, a feature enhancer for cross-modal fusion, a language-guided query selection module for detection-query initialization, and a cross-modality decoder for box refinement. Within decoder layers, detection-queries are fed into a self-attention layer, an image cross-attention layer to combine image features, a text cross-attention layer to combine text features, and an FFN layer. We mainly improve the decoder part, highlighted by the yellow box in Figure 6.

The number prediction head, structured similarly to the detection head with an FFN layer, predicts the number of referred objects from detection-queries. These detection-queries are used to predict the objects, containing number information. The number-queries are learnable embeddings designed to capture various numerical patterns. These queries are initialized randomly with dimensions $(bs, length_nquery, ndim)$, where bs is the batch size, $length_nquery$ represents the number of query lengths, and $ndim$ denotes the feature dimension. The predicted number guides the selection of number-queries through the query selection in Algorithm 1. The selected number-queries have a fixed length of $length_snquery$.

We implement number cross-attention in parallel with self-attention to integrate the number information. In the number cross-attention, the selected number-queries serve as keys and values, while detection-queries serve as queries. The outputs are added to the self-attention features.

4.2. Loss function

For the bounding box supervision, we adopt the loss functions in GDINO [28]. For number prediction, we use L2 loss. To address the challenges posed by varying target counts in real-world scenarios, we quantize the number prediction space into five categories: $\{0, 1, 2, 3, 4+\}$, where $4+$ represents all counts ≥ 4 . Through ablation studies, we set the selected number-queries length ($length_snquery$) to 10 and the number-queries length ($length_nquery$) to 50, corresponding to the five categories.

5. Experiments

5.1. Construction of RDAgent and NGDINO

RDAgent. A straightforward method is to adapt RDAgent for REC tasks. This adaptation automates the process by replacing the object input with predictions from an object detector and removing the human verification step. For a fair comparison, we employ Faster R-CNN [34] as the object detector, which is trained on the VisDrone2019-DET [49] dataset. The agent component utilizes GPT-4o¹.

NGDINO. The NGDINO adopts a two-stage procedure to maintain training stability. First, we pre-train the number

Algorithm 1: Query selection.

```

"""
Input:
detection_queries: (bs, length_dquery, ndim)
number_queries: (bs, length_nquery, ndim)

Output:
selected_number_queries: (bs, length_snquery, ndim)
"""

number_feat = FFN(detection_queries)
# (bs, length_dquery, 1)
number_feat = number_feat.mean(dim=1) # (bs, 1)
number = sigmoid(number_feat) # (bs, 1)
index = slice(length_snquery*number,
              length_snquery*(number+1))
selected_number_queries = number_queries[index]
# (bs, length_snquery, ndim)

```

prediction head on the RefDrone dataset while initializing other components with GDINO [28] parameters. Then, we fine-tune the entire model.

5.2. Implementation details

We establish the benchmark with 13 representative models that can perform REC tasks, comprising 3 specialist models and 10 LMMs. The specialist models include MDETR [14], GLIP [19], and GDINO [28]. For LMMs, we evaluate Shikra [5], ONE-PEACE [38], SPHINX-v2 [21], MiniGPT-v2 [3], Ferret [44], Kosmos-2 [31], Griffon [48], Qwen-VL [1], CogVLM [41], and LLaVA [24]. Detailed model specifications are provided in the Supplementary Material.

Zero-shot evaluation details. For zero-shot evaluation, we use the original model checkpoints as provided in their respective papers. The implementations and checkpoints for GLIP and GDINO are obtained from the MMDetection [4].

Fine-tuning evaluation details. Our fine-tuning protocol maintains consistency across all experiments to ensure a fair comparison. We preserve the original learning strategies while excluding random crop augmentation due to its negative effect on position-sensitive samples. For LMMs, we employ the LoRA [11] fine-tuning strategy and follow the instruction tuning data structures. All fine-tuning experiments run for 5 epochs using 4 NVIDIA A100 GPUs.

5.3. Experimental results

Zero-shot results. Table 2 presents the zero-shot evaluation results, assessing the models’ domain generalization capability. CogVLM [41] demonstrates state-of-the-art performance across multiple metrics. However, several advanced models, including Shikra [5], ONE-PEACE [38], and SPHINX-v2 [21], are limited to outputting only a single bounding box, due to constraints in their pre-training data or output strategy. This restriction significantly impacts their performance in multi-target scenarios.

Fine-tuning results. Table 3 illustrates the fine-tuning per-

¹<https://openai.com/index/hello-gpt-4o/>

Table 2. Experimental results of zero-shot baselines on RefDrone benchmark. Top groups: specialist models. Bottom groups: LMMs for REC tasks. GDINO-T and GDINO-B denote GroundingDINO [28] with Swin-Tiny and Swin-Base backbones. The best results in each group are denoted with **bold**.

Methods	$F1_{inst.}$	$Acc_{inst.}$	$F1_{img.}$	$Acc_{img.}$
MDETR [14]	8.42	4.41	2.99	1.63
GLIP [19]	5.46	3.84	9.20	8.54
GDINO-T [28]	1.18	1.84	3.94	6.35
GDINO-B [28]	1.97	2.23	6.43	7.58
Shikra [5]	0.80	0.52	2.26	1.60
ONE-PEACE [38]	1.02	0.51	2.64	1.34
SPHINX-v2 [21]	1.59	0.80	4.61	2.36
MiniGPT-v2 [3]	2.69	1.36	6.38	3.29
Ferret [44]	3.18	1.62	8.48	4.43
Kosmos-2 [31]	8.06	4.20	8.64	4.52
Griffon [48]	9.16	4.81	16.77	9.18
Qwen-VL [1]	10.91	5.77	18.32	10.08
CogVLM [41]	15.38	8.33	30.73	18.15

Table 3. Experimental results of fine-tuning baselines on Ref-Drone benchmark. Top groups: specialist models. Bottom groups: LMMs for REC tasks.

Methods	$F1_{inst.}$	$Acc_{inst.}$	$F1_{img.}$	$Acc_{img.}$
MDETR [14]	32.60	19.49	19.17	10.81
GLIP [19]	24.23	14.86	16.92	13.29
GDINO-T [28]	30.50	19.02	29.65	21.07
NGDINO-T (Ours)	33.34	20.98	32.45	22.84
GDINO-B [28]	31.96	19.99	31.69	22.26
NGDINO-B (Ours)	34.44	21.76	34.01	23.89
MiniGPT-v2 [3]	4.97	2.74	13.56	8.97
LLaVA [24]	6.00	3.63	14.43	11.57
Qwen-VL [1]	14.14	7.61	20.10	11.17
RDAGENT (Ours)	58.14	41.13	37.07	23.54

formance across different methods. The specialist model MDETR [14] shows strong performance in instance-level metrics, achieving comparable results to GDINO-B [28], but struggles in image-level understanding. Conversely, LMMs like Qwen-VL [1] demonstrate superior image-level comprehension ($F1_{img.}$: 20.10%, $Acc_{img.}$: 11.17%) while struggling with instance-level tasks ($F1_{inst.}$: 14.14%, $Acc_{inst.}$: 7.61%). This performance disparity can be attributed to LMMs’ strong global image understanding capabilities but limited effectiveness in detecting small objects due to input resolution constraints.

The proposed RDAGENT achieves superior results compared to existing approaches, particularly in instance-level metrics, surpassing GDINO-B [28] by 26.18% in $F1_{inst.}$ and 21.14% in $Acc_{inst.}$. The relatively smaller gains in image-level metrics (5.38% in $F1_{img.}$ and 1.28% in

Table 4. Experimental results on gRefCOCO [22] dataset. Asterisk (*) denotes results reported in the gRefCOCO paper.

Methods	testA		testB	
	Pr@0.5 \uparrow	N-acc. \uparrow	Pr@0.5 \uparrow	N-acc. \uparrow
MDETR* [14]	50.0	34.5	36.5	31.0
UNINEXT* [43]	46.4	49.3	42.9	48.2
GDINO-T [28]	45.69	79.02	44.83	76.69
NGDINO-T	46.05	83.17	45.57	78.08

Table 5. Ablation study on RefDrone dataset for the effectiveness of each component in NGDINO, with Swin-Tiny backbone. NPH denotes number prediction head. NCA denotes number cross-attention.

NPH	NCA	$Acc_{inst.}$	$Acc_{img.}$	FPS
		19.02	21.07	13.5
\checkmark		19.09 (0.07 \uparrow)	21.18 (0.11 \uparrow)	12.8 (0.7 \downarrow)
	\checkmark	19.51 (0.49 \uparrow)	21.71 (0.53 \uparrow)	12.9 (0.6 \downarrow)
\checkmark	\checkmark	20.98 (1.96 \uparrow)	22.84 (1.77 \uparrow)	12.3 (1.2 \downarrow)

Table 6. Ablation study for the impact of varying selected number query length. Params indicates additional parameters introduced.

Length	$F1_{inst.}$	$Acc_{inst.}$	$F1_{img.}$	$Acc_{img.}$	Params
1	31.63	19.80	31.23	22.12	1.58M
10	33.34	20.98	32.45	22.84	1.65M
100	32.06	20.10	32.23	22.81	2.34M

$Acc_{img.}$) highlight the importance of instance-level metrics. However, RDAGENT’s multi-step pipeline and reliance on ChatGPT responses result in longer processing time compared to end-to-end approaches.

The proposed end-to-end method, NGDINO, consistently improves over the baseline GDINO [28] across both backbone architectures. Figure 7 shows the visualization results comparing NGDINO and baseline GDINO, demonstrating NGDINO’s effectiveness with multi-target samples.

To further validate the effectiveness of the proposed NGDINO, we conduct additional experiments on the gRefCOCO [22] dataset, which also includes multi-target and no-target samples (Table 4). NGDINO-T outperforms the baseline method GDINO-T, particularly in N-acc. metrics (by 4.15% in test A and 1.39% in test B), which evaluate accuracy on no-target samples. The limited improvements in Pr@0.5 metrics can be attributed to the relatively simple nature of multi-target samples in gRefCOCO, which typically contain only two objects per sample.

5.4. Ablation studies

Ablations of NGDINO components. Table 5 presents the analysis of each component in NGDINO. The number pre-

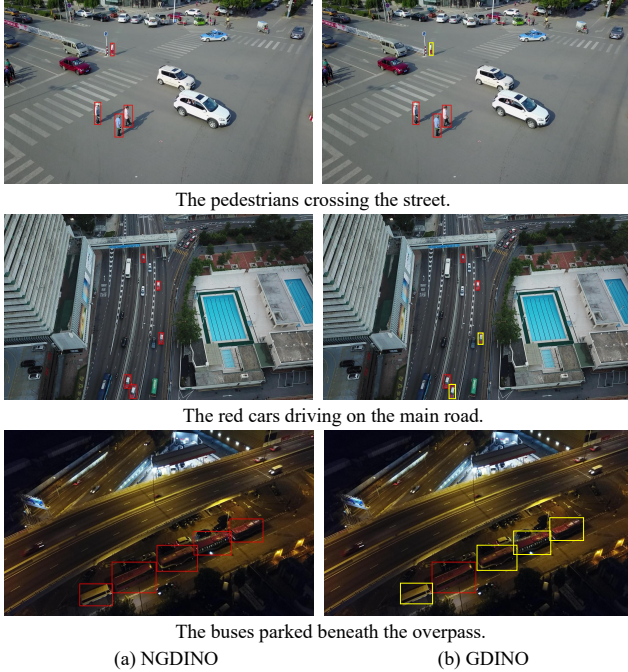


Figure 7. Visualization results comparing NGDINO and GDINO [28], where red boxes indicate true positives and yellow boxes denote false negatives.

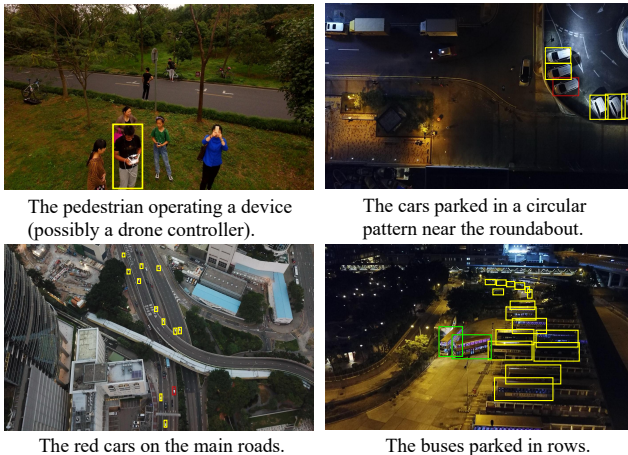


Figure 8. Failure cases of NGDINO on RefDrone dataset. Red, green, and yellow boxes indicate true positives, false positives, and false negatives, respectively.

diction head alone shows a slight increase in $Acc_{inst.}$ from 19.02% to 19.09%, indicating minimal impact of this auxiliary head on the referring tasks. When introducing the number cross-attention without number selection, we observe a more substantial improvement, with $Acc_{inst.}$ increasing from 19.02% to 19.51%. This improvement is attributed to the additional parameters introduced in the decoder. The significant improvement is achieved through the combina-

Table 7. Ablation study for the effectiveness of RDAgent.

Methods	$F1_{inst.}$	$Acc_{inst.}$	$F1_{img.}$	$Acc_{img.}$
ReCLIP [36]	24.62	14.04	11.58	6.15
GPT4-o	52.38	35.65	35.50	22.38
RDAgent	58.14	41.13	37.07	23.54

tion of both the number prediction task and number cross-attention components. This contribution increases $Acc_{inst.}$ from 19.02% to 20.98%. While the additional computational cost results in a minor decrease in inference speed (FPS), this trade-off yields a 1.96% increase in $Acc_{inst.}$.

Ablations of query length. Table 6 analyzes the impact of varying the selected number query length. Utilizing a minimal query length of 1 lacks the capacity to capture complex numerical information. Conversely, extending the query length to 100 increases parameter count and introduces optimization difficulties, thereby adversely affecting performance. Through these experiments, we determine that a query length of 10 provides an optimal trade-off.

Number prediction head performance. The number prediction head achieves an overall number prediction accuracy of 53.5%. During the bounding box prediction stage, this accuracy is observed to be 22.84%. This performance gap demonstrates the effectiveness of number prediction head. Besides, the number prediction achieves a mean absolute error (MAE) of 0.51, suggesting high precision as predictions closely align with ground truth values.

Ablations of RDAgent. Table 7 analyzes the effectiveness of the proposed RDAgent. The GPT4-o baseline is established using only Step 3 of RDAgent. We also compare against ReCLIP [36], a two-stage instance ranking method using CLIP [33] for REC tasks. All experiments utilize Faster-RCNN [34] for object detection. Results show that RDAgent consistently outperforms GPT4-o and ReCLIP across all metrics. However, the performance is partially limited by the Faster-RCNN object detector, which achieves only 18.0 mAP on the VisDrone2019-DET [49] dataset.

5.5. Limitations

While NGDINO addresses the multi-target and no-target challenges, several challenges remain. Figure 8 shows typical NGDINO failure cases, highlighting challenges in the RefDrone dataset. The examples show rich contextual expressions, challenging backgrounds, and small-scale object detection. These challenging cases reflect real-world applications and highlight the areas for future improvement.

6. Conclusion

In this work, we introduce RefDrone, a challenging benchmark specifically designed for referring expression

comprehension in drone scenes. The dataset is constructed using the proposed RDAgent, a semi-auto annotation framework leveraging a multi-agent system. Furthermore, we develop NGDINO to address the multi-target and no-target challenges in the RefDrone dataset. In the future, we aim to further enhance NGDINO to address additional challenges presented by RefDrone. We also plan to expand the benchmark to include referring expression segmentation and referring expression tracking tasks.

References

- [1] Jinze Bai, Shuai Bai, Shusheng Yang, Shijie Wang, Sinan Tan, Peng Wang, Junyang Lin, Chang Zhou, and Jingren Zhou. Qwen-VL: A frontier large vision-language model with versatile abilities. *arXiv preprint arXiv:2308.12966*, 2023. 3, 6, 7
- [2] Wenzhe Cai, Siyuan Huang, Guangran Cheng, Yuxing Long, Peng Gao, Changyin Sun, and Hao Dong. Bridging zero-shot object navigation and foundation models through pixel-guided navigation skill. In *IEEE Int. Conf. Robot. Autom.*, pages 5228–5234, 2024. 1
- [3] Jun Chen, Deyao Zhu, Xiaoqian Shen, Xiang Li, Zechun Liu, Pengchuan Zhang, Raghuraman Krishnamoorthi, Vikas Chandra, Yunyang Xiong, and Mohamed Elhoseiny. MiniGPT-v2: large language model as a unified interface for vision-language multi-task learning. *arXiv preprint arXiv:2310.09478*, 2023. 3, 6, 7
- [4] Kai Chen, Jiaqi Wang, Jiangmiao Pang, Yuhang Cao, Yu Xiong, Xiaoxiao Li, Shuyang Sun, Wansen Feng, Ziwei Liu, Jiarui Xu, Zheng Zhang, Dazhi Cheng, Chenchen Zhu, Tianheng Cheng, Qijie Zhao, Buyi Li, Xin Lu, Rui Zhu, Yue Wu, Jifeng Dai, Jingdong Wang, Jianping Shi, Wanli Ouyang, Chen Change Loy, and Dahua Lin. MMDetection: Open mmlab detection toolbox and benchmark. *arXiv preprint arXiv:1906.07155*, 2019. 6
- [5] Keqin Chen, Zhao Zhang, Weili Zeng, Richong Zhang, Feng Zhu, and Rui Zhao. Shikra: Unleashing multi-modal llm’s referential dialogue magic. *arXiv preprint arXiv:2306.15195*, 2023. 3, 6, 7
- [6] Yue Fan, Winson Chen, Tongzhou Jiang, Chun Zhou, Yi Zhang, and Xin Wang. Aerial vision-and-dialog navigation. In *Findings of ACL*, pages 3043–3061, 2023. 1
- [7] Zhe Gan, Yen-Chun Chen, Linjie Li, Chen Zhu, Yu Cheng, and Jingjing Liu. Large-scale adversarial training for vision-and-language representation learning. *Adv. Neural Inform. Process. Syst.*, 33:6616–6628, 2020. 3
- [8] Chen Gao, Baining Zhao, Weichen Zhang, Jun Zhang, Jinzhu Mao, Zhiheng Zheng, Fanhang Man, Jianjie Fang, Zile Zhou, Jinqiang Cui, Xinlei Chen, and Yong Li. EmbodiedCity: A benchmark platform for embodied agent in real-world city environment. *arXiv preprint arXiv:2410.09604*, 2024. 1
- [9] Zeyu Han, Fangrui Zhu, Qianru Lao, and Huaizu Jiang. Zero-shot referring expression comprehension via structural similarity between images and captions. In *IEEE Conf. Comput. Vis. Pattern Recog.*, pages 14364–14374, 2024. 3
- [10] Richang Hong, Daqing Liu, Xiaoyu Mo, Xiangnan He, and Hanwang Zhang. Learning to compose and reason with language tree structures for visual grounding. *IEEE Trans. Pattern Anal. Mach. Intell.*, 44(2):684–696, 2019. 3
- [11] Edward J Hu, Yelong Shen, Phillip Wallis, Zeyuan Allen-Zhu, Yuanzhi Li, Shean Wang, Lu Wang, and Weizhu Chen. LoRA: Low-rank adaptation of large language models. *Int. Conf. Learn. Represent.*, 2022. 6
- [12] Ronghang Hu, Marcus Rohrbach, Jacob Andreas, Trevor Darrell, and Kate Saenko. Modeling relationships in referential expressions with compositional modular networks. In *IEEE Conf. Comput. Vis. Pattern Recog.*, pages 1115–1124, 2017. 3
- [13] Wei Ji, Li Li, Hao Fei, Xiangyan Liu, Xun Yang, Juncheng Li, and Roger Zimmermann. Towards complex-query referring image segmentation: A novel benchmark. *arXiv preprint arXiv:2309.17205*, 2023. 2, 5
- [14] Aishwarya Kamath, Mannat Singh, Yann LeCun, Gabriel Synnaeve, Ishan Misra, and Nicolas Carion. MDETR-modulated detection for end-to-end multi-modal understanding. In *Int. Conf. Comput. Vis.*, pages 1780–1790, 2021. 3, 6, 7
- [15] Sahar Kazemzadeh, Vicente Ordonez, Mark Matten, and Tamara Berg. Referitgame: Referring to objects in photographs of natural scenes. In *Proc. EMNLP*, pages 787–798, 2014. 2
- [16] Ranjay Krishna, Yuke Zhu, Oliver Groth, Justin Johnson, Kenji Hata, Joshua Kravitz, Stephanie Chen, Yannis Kalantidis, Li-Jia Li, David A Shamma, et al. Visual genome: Connecting language and vision using crowdsourced dense image annotations. *Int. J. Comput. Vis.*, 123:32–73, 2017. 2
- [17] Jungdae Lee, Taiki Miyanishi, Shuhei Kurita, Koya Sakamoto, Daichi Azuma, Yutaka Matsuo, and Nakamasa Inoue. CityNav: Language-goal aerial navigation dataset with geographic information. *arXiv preprint arXiv:2406.14240*, 2024. 1
- [18] Ke Li, Gang Wan, Gong Cheng, Liqiu Meng, and Junwei Han. Object detection in optical remote sensing images: A survey and a new benchmark. *ISPRS journal of photogrammetry and remote sensing*, 159:296–307, 2020. 2
- [19] Liunian Harold Li, Pengchuan Zhang, Haotian Zhang, Jianwei Yang, Chunyuan Li, Yiwu Zhong, Lijuan Wang, Lu Yuan, Lei Zhang, Jenq-Neng Hwang, et al. Grounded language-image pre-training. In *IEEE Conf. Comput. Vis. Pattern Recog.*, pages 10965–10975, 2022. 3, 6, 7
- [20] Tsung-Yi Lin, Michael Maire, Serge Belongie, James Hays, Pietro Perona, Deva Ramanan, Piotr Dollár, and C Lawrence Zitnick. Microsoft COCO: Common objects in context. In *Eur. Conf. Comput. Vis.*, pages 740–755, 2014. 2
- [21] Ziyi Lin, Chris Liu, Renrui Zhang, Peng Gao, Longtian Qiu, Han Xiao, Han Qiu, Chen Lin, Wenqi Shao, Keqin Chen, et al. SPHINX: The joint mixing of weights, tasks, and visual embeddings for multi-modal large language models. *arXiv preprint arXiv:2311.07575*, 2023. 3, 6, 7
- [22] Chang Liu, Henghui Ding, and Xudong Jiang. GRES: Generalized referring expression segmentation. In *IEEE Conf. Comput. Vis. Pattern Recog.*, pages 23592–23601, 2023. 2, 4, 7

- [23] Daqing Liu, Hanwang Zhang, Feng Wu, and Zheng-Jun Zha. Learning to assemble neural module tree networks for visual grounding. In *Int. Conf. Comput. Vis.*, pages 4673–4682, 2019. 3
- [24] Haotian Liu, Chunyuan Li, Qingyang Wu, and Yong Jae Lee. Visual instruction tuning. *Adv. Neural Inform. Process. Syst.*, 36, 2023. 2, 3, 6, 7
- [25] Kehui Liu, Zixin Tang, Dong Wang, Zhigang Wang, Bin Zhao, and Xuelong Li. COHERENT: Collaboration of heterogeneous multi-robot system with large language models. *arXiv preprint arXiv:2409.15146*, 2024. 1
- [26] Shilong Liu, Shijia Huang, Feng Li, Hao Zhang, Yaoyuan Liang, Hang Su, Jun Zhu, and Lei Zhang. DQ-DETR: Dual query detection transformer for phrase extraction and grounding. In *Proc. AAAI Conf. Artif. Intell.*, pages 1728–1736, 2023. 3
- [27] Shubo Liu, Hongsheng Zhang, Yuankai Qi, Peng Wang, Yan-ning Zhang, and Qi Wu. AerialVLN: Vision-and-language navigation for uavs. In *Int. Conf. Comput. Vis.*, pages 15384–15394, 2023. 1
- [28] Shilong Liu, Zhaoyang Zeng, Tianhe Ren, Feng Li, Hao Zhang, Jie Yang, Chunyuan Li, Jianwei Yang, Hang Su, Jun Zhu, et al. Grounding DINO: Marrying dino with grounded pre-training for open-set object detection. *Eur. Conf. Comput. Vis.*, 2024. 3, 5, 6, 7, 8
- [29] Junhua Mao, Jonathan Huang, Alexander Toshev, Oana Camburu, Alan L Yuille, and Kevin Murphy. Generation and comprehension of unambiguous object descriptions. In *IEEE Conf. Comput. Vis. Pattern Recog.*, pages 11–20, 2016. 1, 2
- [30] Kunyu Peng, Jia Fu, Kailun Yang, Di Wen, Yufan Chen, Ruiping Liu, Junwei Zheng, Jiaming Zhang, M. Saquib Sarfraz, Rainer Stiefelhagen, and Alina Roitberg. Referring atomic video action recognition. In *Eur. Conf. Comput. Vis.*, 2024. 2
- [31] Zhiliang Peng, Wenhui Wang, Li Dong, Yaru Hao, Shaohan Huang, Shuming Ma, Qixiang Ye, and Furu Wei. Grounding multimodal large language models to the world. In *Int. Conf. Learn. Represent.*, 2024. 3, 6, 7
- [32] Mengxue Qu, Yu Wu, Wu Liu, Xiaodan Liang, Jingkuan Song, Yao Zhao, and Yunchao Wei. RIO: A benchmark for reasoning intention-oriented objects in open environments. *Adv. Neural Inform. Process. Syst.*, 36, 2023. 2
- [33] Alec Radford, Jong Wook Kim, Chris Hallacy, Aditya Ramesh, Gabriel Goh, Sandhini Agarwal, Girish Sastry, Amanda Askell, Pamela Mishkin, Jack Clark, et al. Learning transferable visual models from natural language supervision. In *Int. Conf. Mach. Learn.*, pages 8748–8763, 2021. 8
- [34] Shaoqing Ren, Kaiming He, Ross Girshick, and Jian Sun. Faster R-CNN: Towards real-time object detection with region proposal networks. *IEEE Trans. Pattern Anal. Mach. Intell.*, 39(6):1137–1149, 2017. 6, 8
- [35] Q. Sima et al. Embodied referring expression for manipulation question answering in interactive environment. In *ICRA*, 2023. 1
- [36] Sanjay Subramanian, Will Merrill, Trevor Darrell, Matt Gardner, Sameer Singh, and Anna Rohrbach. ReCLIP: A strong zero-shot baseline for referring expression comprehension. In *Proc. ACL*, 2022. 3, 8
- [37] Chunlei Wang, Wenquan Feng, Xiangtai Li, Guangliang Cheng, Shuchang Lyu, Binghao Liu, Lijiang Chen, and Qi Zhao. OV-VG: A benchmark for open-vocabulary visual grounding. *Neurocomputing*, 591:127738, 2024. 2
- [38] Peng Wang, Shijie Wang, Junyang Lin, Shuai Bai, Xiaohuan Zhou, Jingren Zhou, Xinggang Wang, and Chang Zhou. ONE-PEACE: Exploring one general representation model toward unlimited modalities. *arXiv preprint arXiv:2305.11172*, 2023. 3, 6, 7
- [39] Tianyu Wang, Haitao Lin, Junqiu Yu, and Yanwei Fu. Polaris: Open-ended interactive robotic manipulation via syn2real visual grounding and large language models. In *International Conference on Intelligent Robots and Systems*, 2024. 1
- [40] T. Wang et al. Embodiedscan: A holistic multi-modal 3d perception suite towards embodied ai. In *CVPR*, 2024. 1
- [41] Weihang Wang, Qingsong Lv, Wenmeng Yu, Wenyi Hong, Ji Qi, Yan Wang, Junhui Ji, Zhuoyi Yang, Lei Zhao, Xixuan Song, et al. CogVLM: Visual expert for pretrained language models. *arXiv preprint arXiv:2311.03079*, 2023. 3, 6, 7
- [42] Chi Xie, Zhao Zhang, Yixuan Wu, Feng Zhu, Rui Zhao, and Shuang Liang. Described object detection: Liberating object detection with flexible expressions. *Adv. Neural Inform. Process. Syst.*, 36, 2023. 2
- [43] Bin Yan, Yi Jiang, Jiannan Wu, Dong Wang, Ping Luo, Zehuan Yuan, and Huchuan Lu. Universal instance perception as object discovery and retrieval. In *IEEE Conf. Comput. Vis. Pattern Recog.*, pages 15325–15336, 2023. 3, 7
- [44] Haoxuan You, Haotian Zhang, Zhe Gan, Xianzhi Du, Bowen Zhang, Zirui Wang, Liangliang Cao, Shih-Fu Chang, and Yinfei Yang. Ferret: Refer and ground anything anywhere at any granularity. *Int. Conf. Learn. Represent.*, 2024. 2, 3, 6, 7
- [45] Licheng Yu, Patrick Poirson, Shan Yang, Alexander C Berg, and Tamara L Berg. Modeling context in referring expressions. In *Eur. Conf. Comput. Vis.*, pages 69–85, 2016. 1, 2
- [46] Sergey Zagoruyko. Wide residual networks. *arXiv preprint arXiv:1605.07146*, 2016. 3
- [47] Yang Zhan, Zhitong Xiong, and Yuan Yuan. RSVG: Exploring data and models for visual grounding on remote sensing data. *IEEE Transactions on Geoscience and Remote Sensing*, 61:1–13, 2023. 2, 5
- [48] Yufei Zhan, Yousong Zhu, Zhiyang Chen, Fan Yang, Ming Tang, and Jinqiao Wang. Griffon: Spelling out all object locations at any granularity with large language models. In *Eur. Conf. Comput. Vis.*, pages 405–422, 2024. 3, 6, 7
- [49] Pengfei Zhu, Longyin Wen, Dawei Du, Xiao Bian, Heng Fan, Qinghua Hu, and Haibin Ling. Detection and tracking meet drones challenge. *IEEE Trans. Pattern Anal. Mach. Intell.*, 44(11):7380–7399, 2021. 2, 3, 4, 6, 8

RefDrone: A Challenging Benchmark for Referring Expression Comprehension in Drone Scenes

Supplementary Material

We provide supplementary material for further analysis, organized as follows:

1. Color attribute analysis of RefDrone. (Appendix A)
2. Details of baseline method. (Appendix B)
3. Additional dataset examples. (Appendix C)
4. Results w.r.t different object scales. (Appendix D)
5. Prompts and examples in RDAgent. (Appendix E)

A. Dataset color attribute analysis

In the RefDrone dataset, color attributes are present in 69% expressions. We initially use the HSV color space to define six primary colors: white, black, red, blue, green, and yellow. During the annotation process, RDAgent expands the color set by adding six more colors: orange, pink, grey, purple, brown, and silver. The distribution of these color terms across the expressions is illustrated in Figure 9.

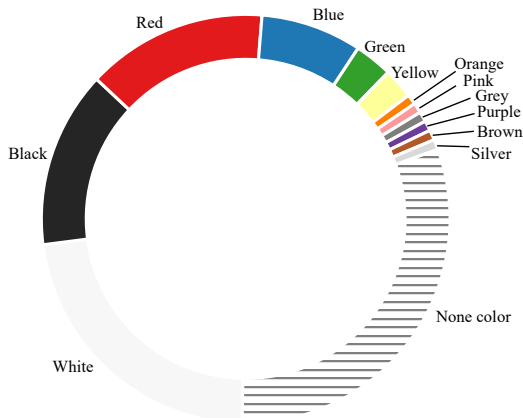


Figure 9. Distribution of color terms in RefDrone expressions.

B. Details of baseline methods

The details for each baseline method:

- *Specialist models:*
 - **MDETR**: ResNet-101 with BERT-Base, pretrained on Flickr30k, RefCOCO+/g, VG.
 - **GLIP**: Swin-Tiny with BERT-Base, pretrained on Object365.
 - **GDINO-T**: Swin-Tiny with BERT-Base, pretrained on Object365, GoldG, GRIT, V3Det.
 - **GDINO-B**: Swin-Base with BERT-Base, pretrained on Object365, GoldG, V3Det.
- *Large multimodal models:*

- **Kosmos-2**: 1.6B parameters.
- **ONE-PEACE**: 4B parameters, visual grounding API.
- **Shikra**: 7B parameters, delta-v1 version.
- **MiniGPT-v2**: 7B parameters.
- **LLaVA**: 7B parameters, v1.5 version.
- **Qwen-VL**: 7B parameters.
- **Ferret**: 7B parameters.
- **CogVLM**: 7B parameters, grounding-specific version.
- **SPHINX-v2, Griffon**: 13B parameters.

C. Dataset examples

To provide a comprehensive understanding of our RefDrone dataset, we present representative examples in Figure 10. These samples demonstrate the three key challenges in our dataset, highlighting its real-world applicability.

D. The results of different object scales.

We add small/medium/large instance accuracy metrics (ACC_s , ACC_m , ACC_l) of RefDrone dataset in Table 8.

Table 8. Fine-tuned results w.r.t. different object scales.

Methods	Acc_s	Acc_m	Acc_l	Methods	Acc_s	Acc_m	Acc_l
GLIP	2.65	18.28	27.29	LLaVA	4.18	7.26	11.99
GDINO-T	8.56	20.66	33.99	Qwen-VL	0.73	10.60	30.18
NGDINO-T	10.84	23.38	40.13	RDAgent	32.54	47.97	47.17

E. Prompts and examples for RDAgent

In this section, we provide the prompts and examples employed in RDAgent. Table 9 presents the prompt construction process for expression generation (Step 3), which includes the system prompt and few-shot in-context learning examples. One in-context learning example is illustrated in Table 10. The system prompts used for each step are detailed in Table 11. Additionally, the system prompts for the feedback mechanism are presented in Table 12.



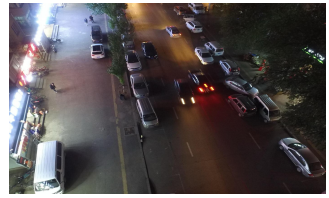
The red cars moving through the intersection.



The yellow dump truck is parked near one of the buildings.



The blue-clad pedestrians are fewer in number and spread out across the area.



The red cars parked along the sides of the road.



The white vehicles waiting at the intersection.



The people on the basketball court.



The white cars park along the road adjacent to the parking lot.



The buses parked in rows within the depot.



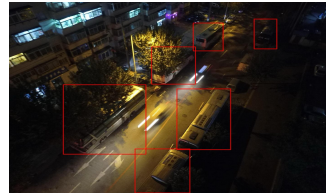
The pedestrians walk along the pathway on the left side of the image.



The red taxi travels on the elevated roadway.



The white cars scattered around the area.



The buses on the road.



The white vans are parked or moving around the intersection.



The pedestrians on the stairs on the left side of the picture.



The white cars park along the road in a line.



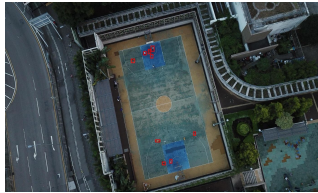
The red cars navigate the intersection.



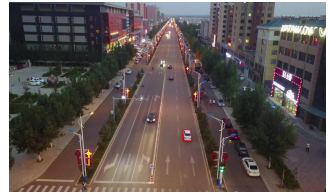
The black cars near each other.



The pedestrians between the bus stop and white bus.



The people playing on the basketball court.



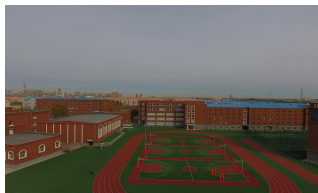
The white cars travel in both directions along the main road.



The red cars in the parking lot.



The black cars parked near the gold building.



Two pedestrians are situated on the right side of the sports field.



The bicycles in the image.

Figure 10. Dataset samples from RefDrone.

Table 9. Illustration of RDAgent’s prompt construction for expression generation (Step 3). Few-shot in-context-learning examples are from [fewshot_samples](#). A representative example is shown in Figure 10

```
messages = [ {"role": "system", "content": f"""As an AI visual assistant, your role involves analyzing a single image. You are supplied with three sentences that caption the image, along with additional data about specific attributes of objects within the image. This can include information about categories, colors, and precise coordinates. Such coordinates, represented as floating-point numbers that range from 0 to 1, are shared as center points, denoted as (x, y), identifying the center x and y. When coordinate x tends to 0, the object nears the left side of the image, shifting towards the right as coordinate x approaches 1. When coordinate y tends to 0, the object nears the top of the image, shifting towards the bottom as coordinate y approaches 1.
```

Your task is to classify the provided objects based on various characteristics, while also substantiating your classification. This classification should be thoroughly justified, with criteria including but not limited to relationships or relative locations of objects.

To refer to a specific object, use the provided coordinates directly. Base your classification justifications on direct observations from the image, avoiding any hypothesizing or assumptions. """ }

```
]
for sample in fewshot_samples:
    messages.append({"role": "user", "content": sample['context']})
    messages.append({"role": "assistant", "content": sample['response']})
messages.append({"role": "user", "content": '\n'.join(query) })
```

Table 10. One example to illustrate the input and output in RDAgent Step 3 (expression generation). The top block shows the input contexts such as image, object, caption and color attributed. The bottom block shows the generated annotations.

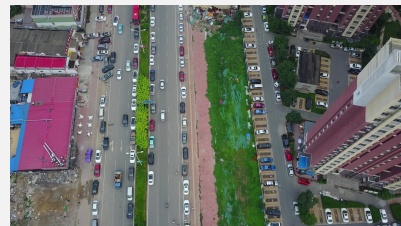
Context type 1: Captions

The image shows an aerial view of a busy urban street with multiple lanes of traffic, flanked by parking areas and buildings. A median strip with greenery runs down the center, dividing the opposite flows of vehicles. On either side of the road, there are commercial and residential structures. Parking lanes on both sides of the main road are filled with parked vehicles.

The image shows a bird’s-eye view of an urban street scene with traffic congestion...{omitted}

Context type 2: Objects

- pedestrian, white: [0.173, 0.849]
- car, black: [0.214, 0.975]
- car, white: [0.215, 0.904]
- car, white: [0.313, 0.444]
- car, red: [0.315, 0.256]
- van, white: ...{omitted}



Context type 3: Image

Response :

The blue cars park on the right parking lot.

Coordinates: [0.628, 0.478], [0.646, 0.692], [0.649, 0.727]

The white cars park on both sides of the main road in a line.

Coordinates: [0.431, 0.051], [0.431, 0.15], [0.431, 0.101], [0.434, 0.256], [0.439, 0.523], [0.443, 0.813], [0.445, 0.902], [0.446, 0.982], [0.235, 0.43], [0.232, 0.486], [0.223, 0.674], [0.215, 0.904]

Table 11. System prompts employed at different stages of RDAgent, replacing the default system messages shown in Table 9

System prompt: Step 1 scene understanding

You are an AI visual assistant that specializes in providing clear and accurate descriptions of images without any ambiguity or uncertainty. Your descriptions should focus solely on the content of the image itself and avoid mentioning any location-specific details such as regions or countries where the image might have been captured.

System prompt: Step 2 color categorization

As an AI visual assistant, your role involves analyzing a single image.

You are supplied with the specific attributes of objects within the image. This can include information about categories, colors, and precise coordinates. Such coordinates, represented as floating-point numbers that range from 0 to 1, are shared as center points, denoted as (x, y) , identifying the center x and y .

Your task is to assess whether the given colors of specific objects match their appearance in the image. Respond with "Yes" when the colors are appropriate. In cases where the colors are deemed inappropriate, respond with a concise "No."

System prompt: Step 3 expression generation

As an AI visual assistant, your role involves analyzing a single image. You are supplied with three sentences that caption the image, along with additional data about specific attributes of objects within the image. This can include information about categories, colors, and precise coordinates. Such coordinates, represented as floating-point numbers that range from 0 to 1, are shared as center points, denoted as (x, y) , identifying the center x and y . When coordinate x tends to 0, the object nears the left side of the image, shifting towards the right as coordinate x approaches 1. When coordinate y tends to 0, the object nears the top of the image, shifting towards the bottom as coordinate y approaches 1.

Your task is to classify the provided objects based on various characteristics, while also substantiating your classification. This classification should be thoroughly justified, with criteria including but not limited to relationships or relative locations of objects.

To refer to a specific object, use the provided coordinates directly. Base your classification justifications on direct observations from the image, avoiding any hypothesizing or assumptions.

System prompt: Step 4 quality evaluation

As an AI visual assistant, your role involves analyzing a single image. You are supplied with three sentences that describe the image, along with additional data about specific attributes of objects within the image. This can include information about categories, colors, and precise coordinates. Such coordinates, represented as floating-point numbers that range from 0 to 1, are shared as center points, denoted as (x, y) , identifying the center x and y . When coordinate x tends to 0, the object nears the left side of the image, shifting towards the right as coordinate x approaches 1. When coordinate y tends to 0, the object nears the top of the image, shifting towards the bottom as coordinate y approaches 1. Besides, you are supplied with the description of the objects and their corresponding attributes.

Your task is to confirm whether the description exclusively relates to the described objects without including any others in the visual. Respond "yes" if it matches, or "no" with an explanation if it does not.

Table 12. RDAgent system prompts for feedback mechanism. Differences from Table 11 are **highlighted**

System prompt: Step 2 color categorization with feedback mechanism

As an AI visual assistant, your role involves analyzing a single image.

You are supplied with the specific attributes of objects within the image. This can include information about categories, colors, and precise coordinates. Such coordinates, represented as floating-point numbers that range from 0 to 1, are shared as center points, denoted as (x, y) , identifying the center x and y .

Your task is to assess whether the given colors of specific objects match their appearance in the image. Respond with "Yes" when the colors are appropriate. In cases where the colors are deemed inappropriate, respond with a concise "No."

System prompt: Step 3 expression generation with feedback mechanism

As an AI visual assistant, your role involves analyzing a single image. You are supplied with three sentences that caption the image, along with additional data about specific attributes of objects within the image. This can include information about categories, colors, and precise coordinates. Such coordinates, represented as floating-point numbers that range from 0 to 1, are shared as center points, denoted as (x, y) , identifying the center x and y . When coordinate x tends to 0, the object nears the left side of the image, shifting towards the right as coordinate x approaches 1. When coordinate y tends to 0, the object nears the top of the image, shifting towards the bottom as coordinate y approaches 1. **You are also provided with descriptions and the objects that initially failed to match, along with the reasons for the discrepancies.**

Your task is to revise both the description and the corresponding objects to correct these mismatches based on the provided reasons. Ensure that the revised description accurately matches the corresponding objects depicted in the visual content.

System prompt: Step 4 quality evaluation with feedback mechanism

As an AI visual assistant, your role involves analyzing a single image. You are supplied with three sentences that describe the image, along with additional data about specific attributes of objects within the image. This can include information about categories, colors, and precise coordinates. Such coordinates, represented as floating-point numbers that range from 0 to 1, are shared as center points, denoted as (x, y) , identifying the center x and y . When coordinate x tends to 0, the object nears the left side of the image, shifting towards the right as coordinate x approaches 1. When coordinate y tends to 0, the object nears the top of the image, shifting towards the bottom as coordinate y approaches 1. **Besides, you are supplied with the description and the objects that initially failed to match.**

Your task is to provide detailed reasoning for unsuccessful object matches.